

# On Coding and Bandwidth Scaling in Ultra-Wideband Communications

Hongsan Sheng, Li Zhao, and Alexander M. Haimovich  
 Department of Electrical and Computer Engineering  
 New Jersey Institute of Technology  
 Newark, New Jersey 07102  
 e-mail: {hs23, haimovic}@njit.edu

*Abstract* — **The information theoretic capacity of a single-user ultra-wideband (UWB) communications is investigated for various modulations under specific UWB regimes: low power spectral density, large spreading ratio, and a highly dispersive channel. We demonstrate that biphasic modulation provides the best performance among several studied formats. The performance loss due to a fixed low coding rate is negligible in the low signal-to-noise ratio (SNR) regime. It is shown that capacity can be obtained by fixing the spreading ratio and allowing the coding rate to vary. However, little is lost by employing a distance-dependent spreading ratio in the presence of a fixed coding rate.**

## I. INTRODUCTION

Impulse radio ultra-wideband (UWB) systems operate across a wide range of the frequency spectrum by sending sequences of short pulses. Employing low duty cycle waveforms, the UWB modulated signal occupies a bandwidth substantially greater than needed, leading to a spread spectrum system [1]. Spreading modulations, such as direct sequence (DS) and pulse position modulation (PPM) with timing hopping (TH) have been proposed for UWB [2, 3].

Due to the low power imposed by regulatory restrictions [4], UWB communications is inherently short range. It is of interest to study the information theoretic channel capacity as a function of the distance between the transmitter and receiver. The large bandwidth available in UWB systems enables not only large spreading ratios, but also very low coding rates. Our goal is to develop an understanding of coding-spreading tradeoff, as well as the role of various parameters in determining the channel capacity of UWB communications.

Coding and bandwidth scaling for spread spectrum communications have been extensively investigated in the literature, for example, [5–8] and references herein. Extending our previous work [9–12], we compute the UWB channel capacity as a function of distance when specific UWB constraints are taken into account. The constraints are the maximum power spectral density (PSD), large but finite bandwidth imposed by the FCC, and a highly dispersive multipath channel [13, 14]. In particular, an outage capacity is investigated accounting for the fading over the multipath channel.

Using capacity expressions constrained by modulation, we compare different modulation schemes combined with ideal coding, and find which signaling is most suitable to UWB. Then, the coding rate is determined at which the loss due to

the constrained signal is negligible. For a fixed coding rate, the achievable information rates are computed as a function of distance. Implied from the channel capacity expressions, the coding rate needs to be adjusted as a function of signal-to-noise ratio (SNR) for best performance. From a practical point of view, it is of interest to assess how much information rate is lost by fixing the coding rate. Moreover, spectrum spreading plays no role in single user case, but decreasing capacity [1]. Due to the low PSD limit, UWB operates in the low SNR regime. In this regime, we seek to determine the conditions under which the capacity loss due to spreading is small. Finally, the outage capacity is investigated in terms of the coding rate, spreading ratio, and delay spread.

The rest of this paper is organized as follows. The next section introduces the system model. In Section III, channel capacity is computed for various signaling inputs. Coding and bandwidth scaling are discussed in Section IV. Conclusions are drawn in Section V.

## II. UWB SYSTEM MODEL

An impulse radio UWB transmission system is shown in Figure 1. The UWB pulse, denoted as  $q(t)$ , has duration  $T_p$ . One symbol is constituted by  $N_p$  pulses. The average pulse interval is  $T_f$ . With  $T_p \ll T_f$ , UWB pulses are transmitted at low duty cycle. DS and PPM with TH are often used in combination with the low duty cycle. It is apparent that UWB is a spread spectrum technique.

A general model of the modulated UWB signal can be expressed

$$s_i(t) = \sum_{j=0}^{N_p-1} p_i(t - jT_f), \quad (1)$$

where  $p_i(t)$  is the UWB waveform determined by the chosen modulation, and  $s_i(t)$  is the  $i$ -th UWB symbol in an  $M$ -ary signal set  $\{s_1(t), s_2(t), \dots, s_M(t)\}$ . The signal bandwidth  $W$  is chosen from a practical UWB proposal [2] to support operation in two bands: a low-band from 3.1 to 4.85 GHz, and a high-band from 6.2 to 9.2 GHz. In [1], such a signal bandwidth  $W$  is called *Fourier bandwidth*, and it is defined as the range of frequencies that encompasses the essential spectral bandwidth occupied by the signal. In [1], the *Shannon bandwidth*,  $B$ , is defined as one-half the minimum number of dimensions ( $N$ ) per second required to represent the signal in a signal space,

$$B = \frac{N}{2T_s}, \quad (2)$$

where  $T_s = N_p T_f$  is the symbol duration. The ratio of the Fourier bandwidth to its Shannon bandwidth is defined as spreading ratio,  $\rho$ ,

$$\rho = \frac{W}{B}. \quad (3)$$

<sup>1</sup>This work was supported in part by NSF award ANI-0338788.

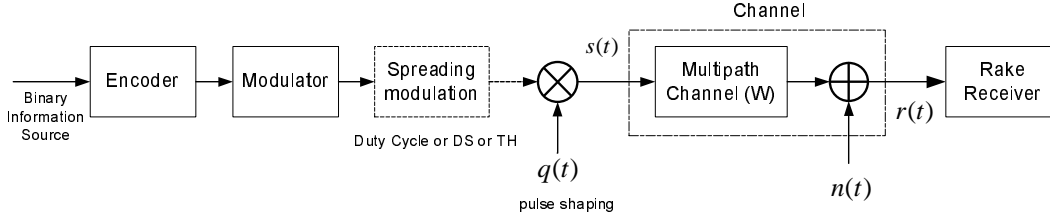


Figure 1: A single user impulse radio UWB transmission system.

By [1], a signal is defined as spread spectrum if  $\rho \gg 1$ .

As shown in Figure 1, a UWB multipath channel can be modeled by the impulse response  $h(t) = \sum_{\ell=0}^{L-1} \alpha_{\ell} \delta(t - \tau_{\ell})$ , where  $L$  is the number of multipath components,  $\alpha_{\ell}$  and  $\tau_{\ell}$  are the  $\ell$ -th path amplitude and delay, respectively, and  $\tau_{\max} = \tau_{L-1} - \tau_0$  serves as the maximum delay spread. The channel statistics are assumed Nakagami- $m$  fading for the distribution of the paths' envelopes [15]. The average received power of the  $\ell$ -th path is expressed  $\Omega_{\ell} = E[\alpha_{\ell}^2] = \Omega \exp[-(\tau_{\ell}/\tau_{L-1}) \delta_0]$ , where  $\Omega$  is chosen such that the total average received power is unity, and  $\delta_0$  is a constant, which determines the power decay factor.

The receiver implements a Rake receiver with  $L$  correlators (fingers), where each finger can extract the signal from one of the multipath components. The outputs of the correlators are combined coherently using maximal ratio combining (MRC). The combiner requires knowledge of the paths' delays and amplitudes. In this work, we assume that the channel state information is perfectly known.

### III. UWB CHANNEL CAPACITY

One question to be answered in this section is, given the PSD constraint, bandwidth, and multipath delay spread, how fast and how far can the information data be transmitted reliably. We start our study of capacity with the additive white Gaussian noise channel, and move on to a multipath channel. We investigate a Gaussian signal input as well as different modulation formats.

#### III.A GAUSSIAN SIGNAL INPUTS

The capacity of the linear Gaussian channel is obtained with a Gaussian distribution of the input signals. The Shannon capacity in bits/sec at a distance  $d$  from the transmitter is

$$C(d) = B \log_2(1 + \text{SNR}(d)) \text{ bits/sec} \quad (4)$$

where  $\text{SNR}(d)$  is the average SNR per dimension at the distance  $d$

$$\text{SNR}(d) = \frac{P_s(d)}{N_0 B} = 2r \frac{E_b}{N_0}(d). \quad (5)$$

In (5),  $P_s(d)$  is the average received signal power per dimension at the distance  $d$  from the transmitter,  $N_0$  is one-sided noise power spectral density,  $E_b/N_0$  is the SNR per bit, and  $r$  is the coding rate measured in bits per dimension

$$r = \frac{R_b}{R_s} \cdot \frac{1}{N}, \text{ bits/dim} \quad (6)$$

where  $R_b$  is the information bit rate in bits/sec, and  $R_s = 1/T_s$  is the symbol rate in symbols/sec, respectively. To account for variations across the bandwidth of the signal,  $P_s(d)$  should be

calculated using the integral of the PSD within a frequency region [12]

$$P_s(d) = \int_{f_L}^{f_H} \frac{S(f)}{L_s(d, f)} df, \quad (7)$$

where  $f_L$  and  $f_H$  are the frequencies measured at the  $-10$  dB emission points,  $S(f)$  is the PSD of the transmitted UWB pulse, and  $L_s(d, f)$  is the wideband frequency-dependent path loss

$$L_s(d, f) = \frac{(4\pi)^2 f^2 d_0^2}{c^2} \cdot \left(\frac{d}{d_0}\right)^n. \quad (8)$$

In (8),  $c$  is the speed of light,  $d_0$  is a close-in reference distance to the transmitter, and  $n$  is path loss exponent. The path loss exponent is  $n = 2$  for line-of-sight (LOS) and  $n = 4$  for non-line-of-sight (NLOS) [14].

#### III.B MODULATED SIGNAL INPUTS

In this section, we compute the capacity for UWB systems when specific modulation formats are employed. Define  $\gamma(d)$  as the SNR per symbol at distance  $d$  from the transmitter

$$\gamma(d) = N \cdot \text{SNR}(d) = 2Nr \frac{E_b}{N_0}(d). \quad (9)$$

For  $M$ -PPM,  $N = M$ , and for biphas and on-off keying (OOK),  $N = 1$ . The  $M$ -PPM channel capacity in bits/sec has been derived in [16] and given by

$$C_{M\text{-PPM}}(d) = \frac{2B}{N} E_{u|s_1} \log_2 \left\{ \frac{N}{1 + \sum_{m=2}^N \exp[-\sqrt{\gamma(d)} u_m]} \right\}, \quad (10)$$

where  $u_m$  is a Gaussian random variable with mean  $\sqrt{\gamma(d)}$  and variance 2. For 2-PPM, (10) becomes [9]

$$C_{2\text{-PPM}}(d) = \frac{B}{\sqrt{\pi}} \int_{-\infty}^{\infty} e^{-x^2} \log_2 \left\{ \frac{2}{1 + e^{-2\sqrt{\gamma(d)} \left[ x + \frac{\sqrt{\gamma(d)}}{2} \right]}} \right\} dx. \quad (11)$$

It can be verified that the channel capacity for biphas modulation is

$$C_{\text{biphase}}(d) = \frac{2B}{\sqrt{\pi}} \int_{-\infty}^{\infty} e^{-x^2} \log_2 \left\{ \frac{2}{1 + e^{-\sqrt{8\gamma(d)} \left[ x + \sqrt{\frac{\gamma(d)}{2}} \right]}} \right\} dx, \quad (12)$$

and for OOK is

$$C_{\text{OOK}}(d) = \frac{2B}{\sqrt{\pi}} \int_{-\infty}^{\infty} e^{-x^2} \log_2 \left\{ \frac{2}{1 + e^{-2\sqrt{\gamma(d)} \left[ x + \frac{\sqrt{\gamma(d)}}{2} \right]}} \right\} dx, \quad (13)$$

respectively, both in bits/sec. Note that  $C_{\text{OOK}}(d) = 2C_{2\text{-PPM}}(d)$ .

In the AWGN channel, to achieve capacity, the UWB pulses have to be placed as close as possible, as long as the corresponding spreading ratio meets the system requirement. However, this situation is not always true over a multipath channel. Due to delay spread from the channel response, interference occurs when the pulse frame time is less than the maximum delay spread. Interference will reduce the capacity. Such interference can be classified into two kinds. One is inter-symbol interference (ISI), which is caused by delay spread of previous symbols. The other interference, referred to as inter-pulse-interference (IPI), occurs between pulses in the same symbol when the system has  $N_p > 1$ . In addition to ISI and IPI,  $M$ -PPM is also subject to self-interference (SI), which occurs when the orthogonality of transmitted PPM symbols is destroyed by the delay spread.

The multipath fading channel parameters  $\{\alpha_\ell, \tau_\ell\}$  are modeled as random variables. Therefore the capacities are also treated as random variables when fading is taken into account. In this case, capacities can be characterized by complementary cumulative distribution function (CCDF). We set a threshold percentage, say, e.g., 90%, and then read from the CCDF graphs the capacity that we can provide with 90% probability. This 90% level amounts to 10% probability of outage [17].

To apply the results in (10)-(13) to the multipath channel, it is needed to replace the SNR in (5) with signal-to-interference-plus-noise ratio (SINR) at the output of the Rake combiner. In practice, Rake receivers often process only a subset of the resolved multipath components ( $L_c$  paths out of the  $L$  resolved multipaths), and combine them using MRC. Such a Rake receiver is referred to as selective. With perfect knowledge of channel parameters  $\{\alpha_\ell, \tau_\ell\}$ , it can be verified that the SINR at the output of the combiner is

$$\text{SINR} = \frac{P_s(d) \left[ \sum_{\ell=0}^{L_c-1} \alpha_\ell^2 \right]^2}{N_0 B \cdot \sum_{\ell=0}^{L_c-1} \alpha_\ell^2 + P_s(d) \sum_{\ell=0}^{L_c-1} \alpha_\ell^2 z_\ell^2}, \quad (14)$$

where  $z_\ell$  represents the interference (ISI, IPI, and/or SI) at the  $\ell$ -th path. Replacing SNR in (9) with (14), and substituting (9) into (10), (11), (12), and (13), we obtain the instantaneous capacity conditioned on each channel realization for  $M$ -PPM, 2-PPM, biphase, and OOK, respectively.

In Figure 2, the capacity with 10% probability of outage for different modulations is plotted as a function of distance  $d$  over a multipath channel. The maximum delay spread is assumed  $\tau_{\text{max}} = 50$  ns. The Nakagami fading parameter is  $m_l = 1$ . Results are shown for the low-band with a spreading ratio  $\rho = 1$ , and the number of selective-Rake fingers  $L_c = 20$ . The UWB capacity in AWGN for different modulations is also shown for comparison.

It is observed that biphase achieves the capacity of Gaussian signaling in AWGN when  $d$  is large (corresponding to the low SNR regime). In multipath situations, biphase has highest outage capacity among other modulations. For short distances (corresponding to the high SNR regime), the outage capacity for  $M$ -PPM is higher than for the other modulations. This is due to the fact that for a fixed bandwidth and a fixed spreading ratio, the symbol duration of  $M$ -PPM is larger than that of biphase and OOK, leading to a reduced effect of the channel delay spread. It is further observed from Figure 2 that the capacity for modulation signals is saturated at short

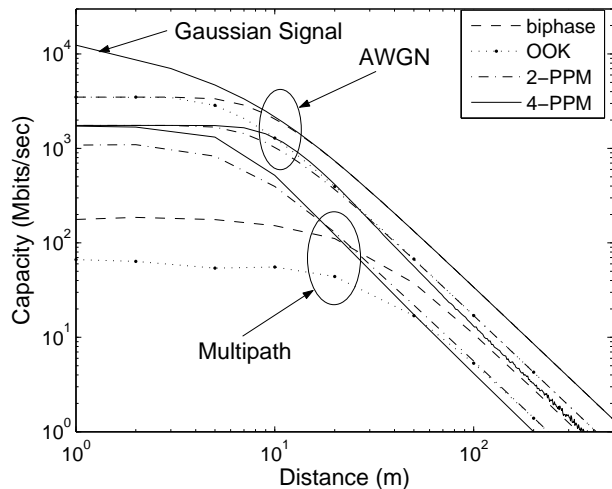


Figure 2: Capacity with 10% outage probability for different signalings as a function of distance over a UWB multipath channel. We assume  $\tau_{\text{max}} = 50$  ns,  $\rho = 1$ , and  $L_c = 20$ .

distances. This is explained as follows. When the transmitter-receiver separation  $d$  becomes small, the SNR is high enough to neglect the effect of noise. From (14), the SINR becomes signal-to-interference ratio (SIR), which is independent of received power  $P_s$ , as well as the distance  $d$ . In this case, the capacity is determined only by the employed modulations and interference.

We have obtained the channel capacity expressions for various modulation signals. Next, we discuss the coding-spreading.

#### IV. CODING AND BANDWIDTH SCALING

In this section, using the expressions derived in the previous section, we investigate the effect of coding and spreading on the capacity. We derive the minimum required  $E_b/N_0$  as a function of coding rate for different modulation schemes. Then we determine the coding rate at which the loss due to the constrained input is negligible, and find the coding gain compared to uncoded modulation. Subsequently, with the coding rate fixed, we vary the spreading gain and compute the achievable information rates as a function of distance. Finally, we determine the conditions under which the loss due to spreading is small.

##### IV.A MINIMUM $E_b/N_0$

We now find the relation between the coding rate and the SNR per bit required for reliable transmission. For a Gaussian signal in AWGN, it can be shown [18]

$$\frac{E_b}{N_0}(r) = \frac{2^{2r} - 1}{2r}. \quad (15)$$

It is seen that  $E_b/N_0$  decreases monotonically with  $r$ . In our case, both  $E_b/N_0$  and  $r$  are implicit functions of the distance  $d$  (both decrease when  $d$  increases, see (5) and (9)). Using an argument similar to the one leading to (15), i.e., letting  $2Br(d) = C(d)$ , we obtain the  $E_b/N_0$  required as a function of  $r$  for various modulation signal inputs, where  $C(d)$  is given

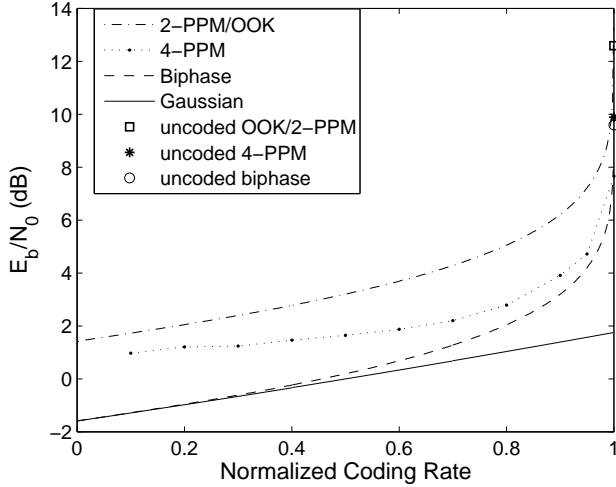


Figure 3: Required  $E_b/N_0$  to obtain a reliable transmission as a function of the normalized coding rate for various signalings.

in (10)-(13). Since no simple closed expression appears to be available, we rely on numerical computations.

In Figure 3, the required  $E_b/N_0$  to obtain a reliable transmission is displayed versus the coding rate for different modulations. To compare the different modulation signals, we define the normalized coding rate

$$r_{\text{norm}} = r \frac{N}{\log_2 M}. \quad (16)$$

It is observed that the Gaussian signal input provides the lower bound for all modulation signals at  $(E_b/N_0)_{\min} = -1.6$  dB. Among modulations, biphase requires lowest  $E_b/N_0$ , while OOK and 2-PPM require highest  $E_b/N_0$ . If the number of orthogonal symbols  $M$  is increased, the required  $E_b/N_0$  approaches the lower bound. It is also shown that a biphase transmission can theoretically achieve the capacity bound at low coding rate, such as  $r \leq 1/4$ . This result is very valuable since the ultra-wideband nature of the signal enables the usage of channel codes with very low coding rates. From (5), the region of  $r \leq 1/4$  corresponds to the low SNR regime for a moderate  $E_b/N_0$ . Note that the required  $E_b/N_0$  for uncoded signals at BER of  $10^{-5}$  is also marked at the abscissa of  $r_{\text{norm}} = 1$ . For a code rate  $r = 1/4$  and biphase signaling, the required  $E_b/N_0$  is  $-0.79$  dB, leading to  $9.59 - (-0.79) \approx 10.4$  dB coding gain.

#### IV.B INFORMATION RATE WITH FIXED CODING RATES

In this section, we estimate the achievable information rates in the presence of a fixed coding rate. From a practical point of view, it is of interest to assess how much information rate is lost by fixing the coding rate. Let the desired coding rate be  $r = r_0$ . A typical value is  $r_0 = 1/4$ . As shown in Figure 3, each modulation requires a  $(E_b/N_0)_{r_0}$  by which reliable communication is possible. As the transmitter-receiver separation increases beyond where the required coding rate is  $r_0$ , the symbol rate needs to be reduced to maintain  $E_b/N_0 = (E_b/N_0)_{r_0}$ . Let  $d_{r_0}$  be the distance at which the required coding rate is

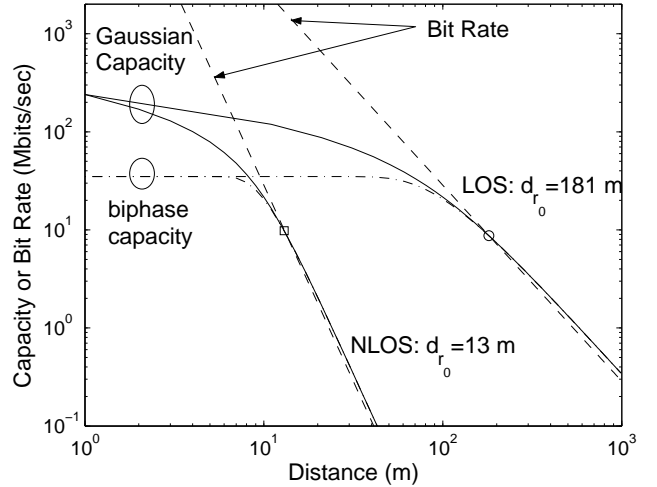


Figure 4: Bit rate and capacity versus distance for Gaussian and biphase inputs at a fixed coding rate  $r_0 = 1/4$ . The spreading ratio is  $\rho = 100$ .

$r_0$ . It can be verified that in AWGN [12]

$$d_{r_0} = \sqrt[n]{\frac{c^2}{(4\pi)^2 N_0 B \cdot 2r_0 \left(\frac{E_b}{N_0}\right)_{r_0}} \int \frac{S(f)}{f^2} df}. \quad (17)$$

Given the path loss exponent  $n$  and pulse waveforms,  $d_{r_0}$  is a function of the Shannon bandwidth,  $B$ .

Turning now to the information rate as a function of distance for a given coding rate. From (5) and (6), we have

$$R_b(d) = \frac{P_s(d)}{N_0 \cdot \left(\frac{E_b}{N_0}\right)_{r_0}}. \quad (18)$$

A few comments are in order with respect to (18). At the distance of  $d_{r_0}$ , we exploit the full Fourier bandwidth of the signal,  $B \stackrel{d_{r_0}}{=} W$ . Using (18) and (6) in (2), the definition of Shannon bandwidth, it follows

$$W = \frac{1}{2r_0} \cdot \frac{P_s(d_{r_0})}{N_0 \cdot \left(\frac{E_b}{N_0}\right)_{r_0}}. \quad (19)$$

As discussed before, at larger distances  $d > d_{r_0}$ , the transmission rate needs to be reduced to maintain a desired performance. Then the Shannon bandwidth decreases. By adjusting the Shannon bandwidth as a function of distance, we maintain a fixed SNR as a function of distance,

$$B(d) = \frac{1}{2r_0} \cdot \frac{P_s(d)}{N_0 \cdot \left(\frac{E_b}{N_0}\right)_{r_0}}. \quad (20)$$

Therefore, substituting (19) and (20) into (3), we obtain a distance-dependent spreading ratio  $\rho(d) = W/B(d) = P_s(d_{r_0})/P_s(d)$ . In conclusion, in the presence of a fixed coding gain, the SNR attenuation with the distance is compensated through a buildup of processing gain.

In Figure 4, we plot the information bit rate versus distance at a fixed coding rate  $r_0 = 1/4$ . The spreading ratio is assumed  $\rho = 100$ . For illustration, only Gaussian and biphase

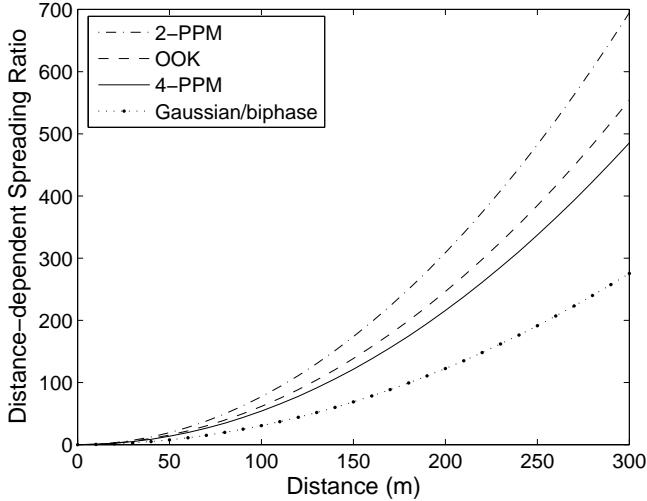


Figure 5: Distance-dependent spreading ratio to maintain a desired  $E_b/N_0$  at a fixed coding rate  $r_0 = 1/4$ .

signaling inputs are shown. Capacity curves are also shown for reference. It is shown that the distance with such a coding rate is  $d_{r_0} = 181$  m for LOS and  $d_{r_0} = 13$  m for NLOS, respectively. When  $d > d_{r_0}$ , the performance loss due to fixed coding rates is negligible.

Figure 5 depicts the needed spreading ratio versus distance for a fixed coding rate  $r_0 = 1/4$ . For brevity, only the result for LOS is plotted. The SNR attenuation with the distance can be compensated by a buildup of a distance-dependent spreading ratio. In conclusion, capacity can be obtained by fixing the spreading ratio and allowing the coding rate to vary. In the presence of a fixed coding rate, capacity can also be achieved by employing a distance-dependent spreading ratio.

It is known that spreading plays no role in single user case, but decreasing capacity. Next, we investigate the effect of spreading on the capacity, and determine the regime that capacity loss due to spreading is small.

#### IV.C CAPACITY LOSS DUE TO SPREADING

When the Shannon bandwidth is substituted with  $W/\rho$ , the channel capacity in (4) can be expressed as a function of spreading ratio

$$C(d) = \frac{W}{\rho} \log_2 \left( 1 + \rho \frac{P_s(d)}{N_0 W} \right), \text{ bits/sec.} \quad (21)$$

Similarly, the capacity expressions in (10)-(13) can be represented in terms of  $\rho$  for modulation signals. For a fixed  $W$ , it is apparent that  $C(d)$  decreases monotonically with increasing  $\rho$ . The loss in capacity due to spreading is defined as

$$\eta = 1 - \frac{C(d)}{\max C(d)}, \quad (22)$$

where the maximum of  $C(d)$  is achieved when  $\rho = 1$ .

Figure 6 depicts the capacity loss as a function of distance for a fixed spreading ratio  $\rho = 100$ . It is observed, when  $d > 15$  m for NLOS, or  $d > 200$  m for LOS, the capacity loss is less than 10%. The region of  $d > 15$  m corresponds to the low SNR regime. This is true for all modulated signals. This

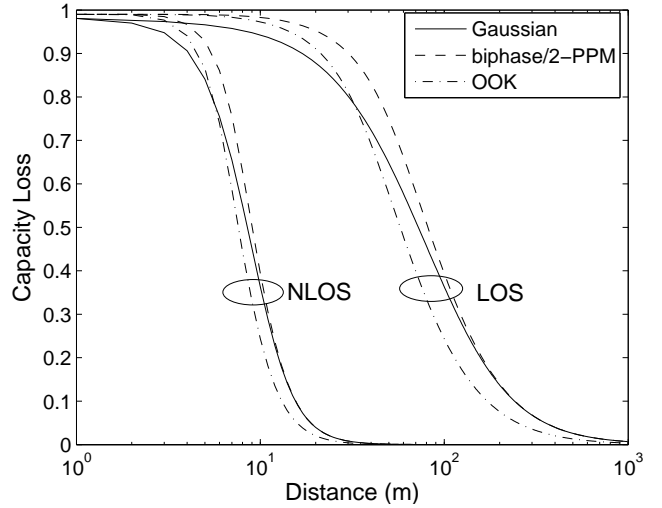


Figure 6: Capacity loss as a function of transmission distance for a given spreading ratio  $\rho = 100$ .

result clearly demonstrate that, in the low SNR regime (corresponding to a large distance), capacity loss due to spreading is small.

In a multipath channel, the outage capacity is a function of the spreading ratio and delay spread. This is shown in Figure 7. We compare the capacity with 10% outage probability versus spreading ratio for different modulated signals. We assume  $\tau_{\max} = 50$  ns,  $L_c = 20$ , and  $d = 100$  m. It is seen that a largest outage capacity exists when the spreading ratio increases. In general, a larger  $\rho$  value is associated with a longer symbol duration  $T_s$ , and less interference. Consequently, the effective SINR is higher, leading to a higher capacity. On the other hand, a longer  $T_s$  corresponds a lower transmission rate  $R_s$ , resulting in a lower capacity.

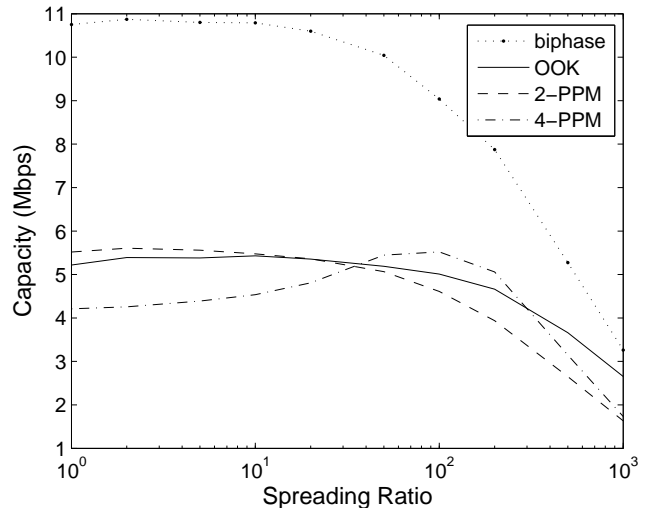


Figure 7: Capacity with 10% outage probability over a multipath fading channel as a function of spreading ratio for different signaling inputs. We assume  $\tau_{\max} = 50$  ns,  $d = 100$  m and  $L_c = 20$ .

## V. CONCLUSION

The channel capacity for UWB systems was investigated for different signaling formats under specific UWB regimes: low PSD limitation, large spreading ratio, and high delay spread. In particular, outage capacity over a UWB multipath fading channel was computed as a function of spreading ratio and delay spread. Different modulation schemes using ideal coding were compared in terms of required SNR per bit. It was shown that biphasic modulation provided the best performance among several studied modulation formats. Effects of coding and spreading on the channel capacity were then discussed, and the region suitable to UWB operations was determined. It was demonstrated that, in low SNR regime ( $d > 13$  m at NLOS), the performance loss in the presence of a fixed coding rate was negligible. For a fixed coding rate, the SNR attenuations with distance was compensated using a distance-dependent spreading ratio. In the low SNR regime ( $d > 15$  at NLOS), the capacity loss due to spreading was small.

## REFERENCES

- [1] J. L. Massey, "Towards an information theory of spread-spectrum systems," in *Code Division Multiple Access Communications*, S. G. Glisic and P. A. Leppnen, Eds. Boston, Dordrecht and London: Kluwer, 1995, pp. 29–46.
- [2] R. Fisher, M. McLaughlin, M. Welborn, *et al.* (2004, July) DS-UWB Physical Layer Submission to 802.15 Task Group 3a. [Online]. Available: <ftp://ieeewireless@ftp.802wirelessworld.com/15/04/15-04-0137-03-003a-merger2-proposal-ds-uwb-update.doc>
- [3] M. Z. Win and R. A. Scholtz, "Ultra-wide bandwidth time-hopping spread-spectrum impulse radio for wireless multiple-access communications," *IEEE Trans. Commun.*, vol. 48, no. 4, pp. 679–691, Apr. 2000.
- [4] (2002, Feb.) Revision of Part 15 of the commission's rules regarding ultra-wideband transmission systems. First Report and Order. Federal Communications Commission. ET Docket 98-153, FCC 02-48.
- [5] M. Médard and R. G. Gallager, "Bandwidth scaling for fading multipath channels," *IEEE Trans. Inform. Theory*, vol. 48, no. 4, pp. 840–852, Apr. 2002.
- [6] S. Verdú, "Spectral efficiency in the wideband regime," *IEEE Trans. Inform. Theory*, vol. 48, no. 6, pp. 1319–1343, June 2002.
- [7] V. V. Veeravalli and A. Mantravadi, "The coding-spreading tradeoff in CDMA systems," *IEEE J. Select. Areas Commun.*, vol. 20, no. 2, pp. 396–408, Feb. 2002.
- [8] D. Porrat and D. N. C. Tse, "Bandwidth scaling in ultra wide-band communications," in *Proc. Annual Allerton Conference on Commun., Control, and Computing*, Oct. 2003.
- [9] L. Zhao and A. M. Haimovich, "Capacity of M-ary PPM ultra-wideband communications over AWGN channels," in *Proc. IEEE Semiannual Veh. Technol. Conf. (VTC)*, vol. 2, Atlantic City, New Jersey, Fall, 2001, pp. 1191–1195.
- [10] —, "The capacity of an UWB multiple-access communications system," in *Proc. IEEE Int. Conf. Commun.*, vol. 3, Apr. 2002, pp. 1964–1968, New York, NY.
- [11] L. Zhao, A. M. Haimovich, and M. Z. Win, "Capacity of ultra-wide bandwidth communications over multipath channels," in *Proc. IEEE International Symposium on Advances in Wireless Communications (ISWC'02)*, Victoria, Canada, Sept., 23–24 2002.
- [12] H. Sheng, P. Orlik, A. M. Haimovich, L. Cimini, and J. Zhang, "On the spectral and power requirements for ultra-wideband transmission," in *Proc. IEEE Int. Conf. Commun. (ICC'03)*, vol. 1, Anchorage, AK., May 2003, pp. 738–742.
- [13] IEEE P802.15 Working Group for Wireless Personal Area Networks (WPANs). (2003, Feb.) Channel modeling sub-committee report final. [Online]. Available: <http://www.ieee802.org/15/pub/2003/Mar03/02490r1P802-15-SG3a-Channel-Modeling-Subcommittee-Report-Final.zip>
- [14] IEEE P802.15 Study Group 4a for Wireless Personal Area Networks (WPANs). (2004, Sept.) IEEE 802.15.4a channel model subgroup final report. [Online]. Available: <ftp://ieeewireless@ftp.802wirelessworld.com/15/04/15-04-0535-00-004a-tg4a-channel-model-final-report.pdf>
- [15] D. Cassioli, M. Z. Win, and A. F. Molisch, "The ultra-wide bandwidth indoor channel: from statistical model to simulations," *IEEE J. Select. Areas Commun.*, vol. 20, no. 6, pp. 1247–1257, Aug. 2002.
- [16] S. Dolinar, D. Divsalar, J. Hamkins, and F. Pollara, "Capacity of pulse-position modulation (PPM) on Gaussian and Webb channels," JPL TMO, Tech. Rep. 42-142, August 15, 2000.
- [17] G. J. Foschini and M. J. Gans, "On limits of wireless communications in a fading environment when using multiple antennas," *Wirel. Pers. Commun.*, vol. 6, no. 3, pp. 311–335, 1998.
- [18] S. Benedetto and E. Biglieri, *Principles of Digital Transmission: with Wireless Applications*. Kluwer Academic Publishers, 1999.